Proceedings of the ASME 2010 3rd Joint US-European Fluids Engineering Summer Meeting and 8th International Conference on Nanochannels, Microchannels, and Minichannels
FEDSM-ICNMM2010
August 1-5, 2010, Montreal, Canada

FEDSM-ICNMM2010-31098

NUMERICAL SIMULATION OF CONFINED NANO-IMPINGING JET IN MICROSCALE COOLING APPLICATION USING DSMC METHOD

M. Darbandi[1], darbandi@sharif.edu
H. Akhlaghi[2], hassan.akhlaghi@gmail.com
A. Karchani[3], abolfazl.karchani@gmail.com
[1,2,3] Department of Aerospace Engineering, Sharif University Of Technology, Tehran, Tehran, Iran 11365-11155

G.E. Schneider[4], gerrys@uwaterloo.ca
[4]Department of Mechanical and Mechatronics Engineering, University Of Waterloo Ontario, Waterloo, ON, Canada CPH-3678

ABSTRACT

In this study, we simulate rarefied gas flow through a confined nano-impinging jet using direct simulation Monte Carlo (DSMC) method. The effects of geometrical parameters, pressure ratio, and wall conditions on the heat transfer from a hot surface are examined. Hot surface modeled via diffusive constant wall temperature. Various inlet/confining surface conditions such as specular, adiabatic, and constant temperature are implemented and the effects of them on the wall heat flux rates are studied. The results show that Knudsen number, velocity slip, and temperature jump are main reasons which specify magnitudes of wall heat flux rates. Among all geometrical parameters, H/W ratio has the greatest effect on heat transfer, where H is jet distance from the hot surface and W is the jet width. For different values of pressure ratio, the biggest quantity of wall heat flux rate relates to the lowest velocity slip case. Also for inlet/confining walls with constant temperature condition equal to coolant flow temperature, heat transfer from the hot surface was the maximum.

1. INTRODUCTION

With a fast progress in nanotechnology devices and components, a fundamental understanding of the heat transfer phenomena in nanochannels has become so critical for the systematic design and precise control of such miniaturized devices towards the integration and automation of Lab-on-a-chip devices [1]. Indeed, the quantity of energy needs to be dissipated by the cooling systems of nano-electronic components increases steadily. In one hand, micro- and nano-electronic components are decreasing in dimension and in another hand, the devices power consumption is increasing. Therefore, a question about the ways they need to be cooled emerges important [2]. Miniaturization of MEMS and NEMS devices requires advanced understanding of micro and nano scale flow and heat transfer physics. This is due to the fact that the fluid flow behavior at tiny scales is fundamentally different from that at macroscopic scales as the characteristic length scales of micro-devices may be closed to the mean-free-path of the gas (λ) [3]. In rarefied flows, the mean free path of the molecules λ, is same order as the flow length scale H. For such flows, the ratio of λ/H, commonly referred to as the Knudsen number, is high and the fluid motions are better described from the molecular point of view [4]. In these flows, Reynolds number is rather low in the order of 10 and the viscous force is dominant over the inertial force. Therefore, the viscous transport of momentum and heat may become an important aspect of such flows [5]. The DSMC method is a molecular approach where the continuum assumption breaks down. The DSMC method is a numerical method, which is applied to simulate the flow in a physical way based on a molecular model. In this model, the state of the flow is determined by the positions and the velocity components of the representative molecules [6].

Because of the high heat transfer rates, using from cooling impinging jets has been increased in recent decades. Approximately, all previous numerical and experimental of impinging jets are limited to the continuum flows for milli-impinging jets [7-21]. Some literatures studied turbulence modeling in impinging jet flows [7-14]. In these researches, Reynolds number ranges from 20000 to 70000 and they are focused on turbulence modeling. Some literatures have worked experimentally on impinging jet flow and present correlations for Nusselt number [15-21]. A recent work done by Kursun and Kapat [22] is the basis of present work. Kursun and Kapat studied a micro slot impinging jet using DSMC-IP method. They studied rarefied coolant gas flow through a slot impinging jet with constant pressure ratio at the inlet/outlet boundaries. They used constant wall heat flux as a hot surface and compare two cases with different dimensions. In their work, they concentrated on IP method and there were no detailed study on heat transfer characteristics.

In this study, we examine the effects of flow and geometrical parameters on heat transfer characteristics using DSMC method. The geometry and inlet/outlet flow conditions in our research is same as Kursun and Kapat's work [22]. Influence of different wall configurations and inlet/outlet flow conditions are investigated. Nitrogen gas is used as coolant fluid. Following Wang and Li [23], we use the 1D characteristics theory to apply inlet/outlet pressure boundary conditions.

2. GOVERNING EQUATIONS

To formulate the molecular motions in a flow, Maxwell suggested a velocity distribution function $f(c)$ to describe the probability of a molecule to have a certain velocity at a certain location and time. Due to molecular chaos in a dilute gas, it is possible to use a velocity distribution function for a single molecule. Other macroscopic quantities can be calculated using this velocity distribution function. The Boltzmann equation describing the time evolution of the velocity distribution function of molecules is given by

$$\frac{\partial}{\partial t}(nf)+c\frac{\partial}{\partial r}(nf)+F\frac{\partial}{\partial c}(nf)= \int_{-\infty}^{\infty}\int_{0}^{4\pi} n^2(f^*f_1^*-ff_1)c_r\sigma\, d\Omega dc_1 \tag{1}$$

where n is number density, t is time, r is space vector, c is velocity space vector, F is external force per unit mass, c_r is the relative velocity between a molecule of velocity class c and one with velocity class c_1 , $\sigma\, d\Omega$ is differential cross-section for the collision of a molecule of class c with another one having class c_1 such that their post-collision velocities are c^* and c_1^*, respectively, and functions f, f_1, f^* and f_1^* are the corresponding velocity distribution functions for the molecule and its collision partner before and after the collisions. Equation (1) is a seven-dimensional integro-differential equation. The first term describes the change rate of the number of molecules. The second and third terms describe the changes of the number of molecules due to molecular movement and due to an external force field. The term on the right hand side is called the collision integral term, which causes major difficulty to solve this equation. This term describes the change of molecular velocities after molecular collisions.

3. THE DSMC APPROACH

The DSMC method was first introduced by Bird [6] to study rarefied gaseous flows. This method consists of indexing molecules into cells, tracking the movements of molecules, selecting collision pairs, and calculating postcollision properties. Computational domain is divided into a number of cells. Each cell contains a number of subcells which used for selecting collision pairs. The DSMC method has two distinct traits; first, each simulated particle is representative of a large number of real molecules in DSMC method, and second, molecular motion and molecular collision are decoupled by a computational time step. This time step is smaller than physical collision time and will set such that a typical molecule moves remains in a cell in several time steps. In present simulations, time step has been chosen such that a typical molecule moves about one fourth of the cell dimension in one computational time step. The variable hard sphere (VHS) has been applied as a collision model in all the simulations. By this model, intermolecular potential between collision pairs are simulated and post-collision velocities are calculated. For equilibrium gases, the temperature can be calculated from [6]:

$$T=\left(3T_{tr}+\zeta_r T_{rot}\right)/\left(3+\zeta_r\right) \tag{2}$$

where the molecular vibrational energy is neglected. T_{tr} and T_{rot} are translational and rotational temperatures, respectively. They can be determined using parameters such as Boltzman constant K, molecular mass m, molecular velocity c, mean velocity of simulated molecules c_0, number of rotational degrees of freedom ζ_r, rotational energy of an individual molecule, which yield:

$$\frac{3}{2}KT_{tr}=\overline{mc^2}-\overline{m}c_0^2 \tag{3}$$

$$T_{rot}=\left(2/k\right)\left(\overline{\varepsilon_{rot}}/\zeta_r\right) \tag{4}$$

The over bar variables represent sample averaging values. According to the above equations, gas temperature depends on velocity magnitude and rotational energy of particles. The net heat flux on the wall per unit width can be evaluated from:

$$q=\frac{\left[\left(\sum_{i=1}^{n}\varepsilon_{tr}+\sum_{i=1}^{n}\varepsilon_{rot}\right)_{inc}-\left(\sum_{i=1}^{n}\varepsilon_{tr}+\sum_{i=1}^{n}\varepsilon_{rot}\right)_{ref}\right]N_0}{\Delta t\left(1.\Delta x\right)} \tag{5}$$

where n is total number of simulated molecules that strike the wall during the sampling, N_0 is number of gaseous molecules associated with one computational molecule, and Δt is time period of the sampling. In fact, the wall heat flux rate is based on difference in incident and reflected molecules.

4. BOUNDARY CONDITIONS

All boundary conditions in DSMC can be devided in two main classes. Class one that contains flow boundaries in which molecules enter or exit from the domain and class two that represents surface conditions.

4.1 SUBSONIC BOUNDARY CONDITION

In the DSMC method, all three flow parameters, i.e., density, temperature and velocity must be specified for incoming molecules at the inlet/outlet boundaries. For high speeds flows, such as hypersonic flows, the thermal velocity can be smaller in magnitude compared with the mean velocity. For a DSMC simulation of high-speed flow, a conventional approach is to impose a ''vacuum'' condition at the exit boundary, where no molecules enter the computational domain from the region external to the flow domain. For the low-speed flows in fluidic MEMS, the thermal motion can be of the same order of magnitude as the mean molecular motion. It then becomes inappropriate to neglect the mass influxes at a flow boundary [24]. Liou and Fang [25] proposed an implicit boundary treatment for low speed MEMS flow simulations. In this method, the number of molecules entering the computational domain and their corresponding internal energy

and velocity components are determined in an implicit manner by the local mean flow velocity, temperature, and number density. The number flux of the molecules entering the computational domain described by using the Maxwellian distribution function [24],

$$F_j = \frac{n_j}{2\sqrt{\pi}\beta_j}\left[\exp\left(-s_j^2\cos^2\nu\right)+ \sqrt{\pi}s_j\cos\nu\left\{1+\mathrm{erf}\left(s_j\cos\nu\right)\right\}\right] \tag{6}$$

where,

$$S_j = U_j\beta_j \tag{7}$$

$$\beta_j = 1/\sqrt{2RT_j} \tag{8}$$

F_j represents the number flux through a cell face of the boundary cell *j*-th. ''erf'' denotes the error function, R the gas constant, and n_j the number density of molecules in cell *j*-th. T_j and U_j denote the local temperature and the streamwise mean velocity component, respectively. The value of v is zero for the upstream boundary and π for the downstream exit boundary.

Velocity components of the entering molecule determined by using the acceptance-rejection method [4] and the Maxwellian distribution function. At the upstream inlet boundary, the streamwise velocity u and cross-stream velocities, v and w, of the molecules entering the computational domain through the cell face of a boundary cell *j* can be written as:

$$\begin{aligned} u &= \left(U_{j,in} + 3C_{mp}\right)R_f \\ v &= A\cos\left(\varphi\right)+V_{j,in} \\ w &= A\sin\left(\varphi\right) \end{aligned} \tag{9}$$

where,

$$\begin{aligned} A &= \sqrt{-\ln\left(R_f\right)}C_{mp} \\ \varphi &= 2\pi R_f \\ C_{mp} &= \sqrt{2RT_j} \end{aligned} \tag{10}$$

R_f represents a random fraction number, and C_{mp} the local most probable thermal speed of molecules. At the downstream, the velocity components for the molecule entering the computational domain through the exit flow boundary are:

$$\begin{aligned} u &= \left(U_{j,out} - 3C_{mp}\right)R_f \\ v &= A\cos\left(\varphi\right)+V_{j,out} \\ w &= A\sin\left(\varphi\right) \end{aligned} \tag{11}$$

where $V_{j,out}$ denotes the exit local transverse mean velocity. With the vibrational energy neglected, the internal energy of the entering equilibrium gases of diatomic molecule consists of translational energy, e_{tr}, and rotational energy e_{rot}:

$$\begin{aligned} e_{tr} &= mc^2/2 \\ e_{rot} &= -\ln\left(R_f\right)KT_j \end{aligned} \tag{12}$$

where c is the speed of an entering molecule, m the mass of the simulated gas, and K the Boltzmann constant.

In order to implement equations (5)–(11), the number density, temperature, and mean velocity at the flow boundaries are needed. At the upstream boundary, the pressure, P_{in}, and density, T_{in}, are the given parameters of the flow. The temperature, ρ_{in}, can be obtained according to the equation of state. That is:

$$\begin{aligned} \rho_{in} &= P_{in}/\left(T_{in}R\right) \\ n_{in} &= \rho_{in}/m \end{aligned} \tag{13}$$

Liou and Fang [25] used a first-order extrapolation to determine the streamwise mean velocity, $U_{j,in}$, from that of the computed for cell *j*-th. That is:

$$U_{j,in} = U_j \tag{14}$$

The transverse mean velocity, $V_{j,in}$, is set zero. This method is easy to use. However, Wang and Li [23] showed it takes a long time to converge because the velocity of coming particles does not embody the pressure information. It also shows that this treatment has some difficulties when the wall temperature is quite different from the gas temperature. They proposed another treatment for the upstream pressure boundary based on the theory of characteristics [23]:

$$\begin{aligned} U_{j,in} &= U_j + \left(P_{in}-P_j\right)/\left(\rho_i a_i\right) \\ V_{j,in} &= V_j \end{aligned} \tag{15}$$

In above, a_j is the local inlet speed of sound. At the downstream boundary, the only given flow parameter is the outlet pressure, P_{out}. The other mean properties of the flow are to be determined implicitly as the calculation proceeds. In implicit boundary method [24], the flow variables are first computed by the following characteristics-theory-based equations:

$$\begin{aligned} \rho_{j,out} &= \rho_j + \left(P_{out}-P_j\right)/a_j^2 \\ U_{j,out} &= U_j + \left(P_j-P_{out}\right)/\left(\rho_j a_j\right) \\ V_{j,out} &= V_j \\ T_{j,out} &= P_{out}/\left(\rho_{j,out}R\right) \end{aligned} \tag{16}$$

The subscript *out* denotes the exit boundary.

4.2 WALL BOUNDARY CONDITION

We use the diffuse reflection model at the solid walls. In this model, the emission of impinging molecules is not correlated with the pre-impingement state of the molecules. The outgoing velocity of molecules is randomly assigned according to a half-range Maxwellian distribution determined by the wall temperature. This is also known as the full thermal and momentum accommodation. For a wall aligned in y direction:

$$u = \sqrt{-\ln(R_f)}C_{mp}\sin(2\pi R_f)$$

$$v = \sqrt{-\ln(R_f)}C_{mp} \qquad (17)$$

$$w = \sqrt{-\ln(R_f)}C_{mp}\cos(2\pi R_f)$$

In above equation, the most probable speed calculated by wall temperature:

$$C_{mp} = \sqrt{2RT_w} \qquad (18)$$

The temperature at the upper and lower walls of microchannel is uniform.

5. RESSULTS AND DISCUSSION

First, we would like to verify the extended DSMC solver in the application of Impingement jet flow simulation. As was mentioned in the introduction section, Ref. [22] is the only DSMC work in the simulation of rarefied impinging flow. Therefore, we evaluate our DSMC solver by solving the pressure-driven impingement flow under constant wall heat flux rate. Our results can be compared with those presented in Kursun and Kapat [22]. We apply the inverse temperature sampling (ITS) technique [26] to implement constant heat flux equal 1.46×10^5 on the wall.

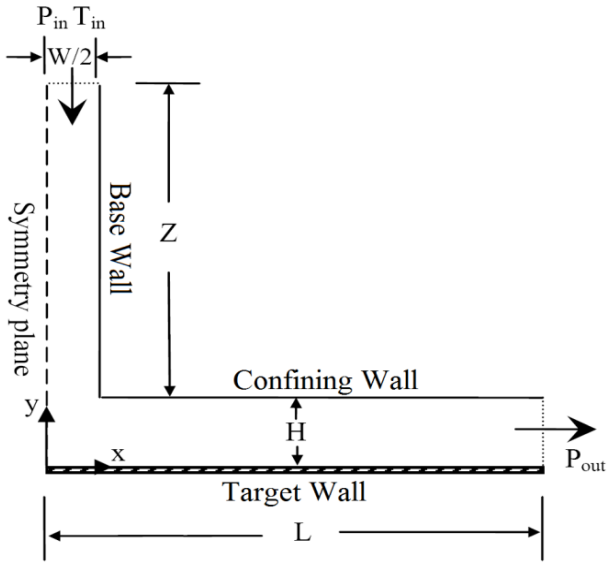

Figure 1. The geometry of impinging jet and the imposed boundary conditions.

Figure 1 shows a schematic of computational domain. The geometry has consisted of three wall surface such as base, confining, and target wall. Base or inlet wall is used slot impinging jet application [16, 22]. Inlet flow with pressure of 2 atmospheres and temperature of 300 K enter to the computation domain. Back pressure is set to the atmospheric condition. In this test case, confining wall has a temperature equal to the inlet flow. Figure 2 shows the Nusselt number distribution on the target wall compared with Ref. [22]. The results approximately have a good agreement with those of Ref. [22], but there are some differences. These differences may be due to two factor; first, we use DSMC method and they used DSMC-IP method, and second, they did not mention how implement constant wall heat flux on the wall. According to the Fig. 2, we can conclude that the developed DSMC solver is reliable enough to launch our study further.

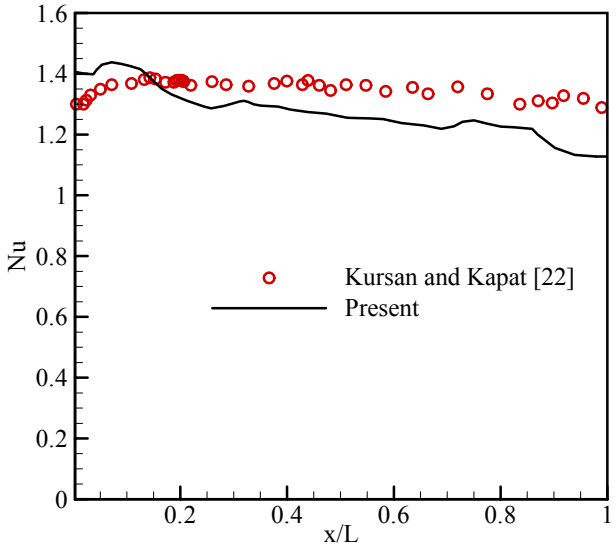

Figure 2. Nusselt number distribution on the wall compared with Ref. [22]

Table 1. The details of chosen test cases

Case	H (μm)	W (μm)	P_i/P_o	Inlet Wall	Confining Wall
1	0.6	2.4	2	Specular	Diffusive (T_{CW} = 300K)
2	1.2				
3	2.4				
4	4.8				
5	9.6				
6	2.4	1.2			
7		2.4			
8		4.8			
9		2.4	1.5		
10			2		
11			3		
12			4		
13			5		
14	0.6	2.4	2	Diffusive (T= 300K)	
15				Specular	
16				Adiabatic	

We study different cases to elaborate the resulting flow behavior and heat transfer characteristics from a hot surface by a confined impinging jet. They are summarized in Table 1. In all of our studies, we consider nitrogen as the coolant fluid. One half of the geometry is simulated due to the symmetric flows

and cell width considered as 0.8 λ. In all cases, lengths of target plate and inlet channel are set to 2L=18μm and Z=1.8μm respectively. Also Temperature of coolant flow and hot surface are 300K and 360K respectively.

At the first, we want to examine the effects of geometrical parameter on the flow configuration and heat transfer. In Cases 1-5, jet distance from the wall increases from 0.6 to 9.6 μm. Figure 2 shows the flow configuration and Mach contours for different jet distance from the wall. According to the figure, flow speed increases as jet distance from the wall increases. It leads to stronger vortex at the domain. This is mainly due to increasing of the cross section area.

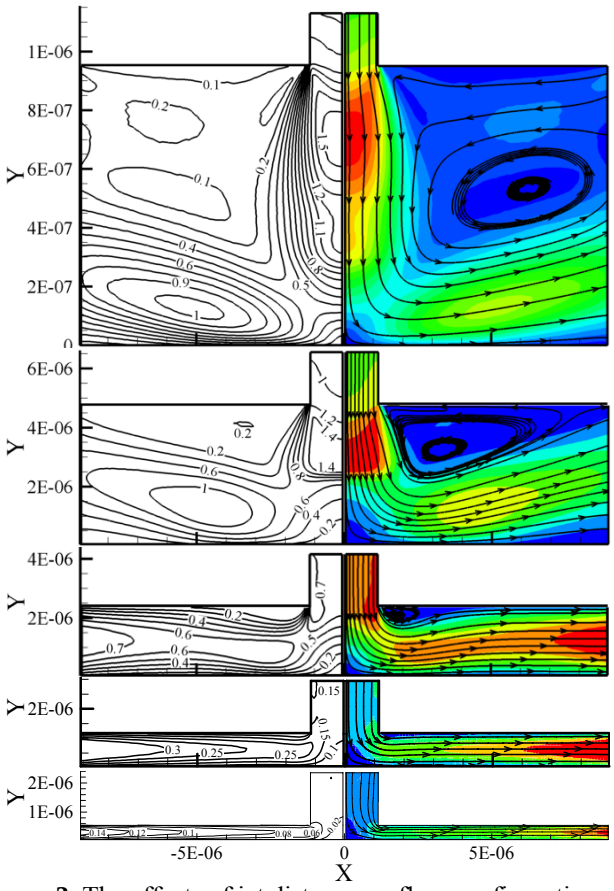

Figure 3. The effects of jet distance on flow configuration and Mach contours, Cases 1-5.

Variation of averaged wall heat flux rates for different jet distance from the wall (Cases 1-5) are showed in figure 4. According to the results, averaged values of wall heat flux rates decrease as the jet distance increases. It is because of the decreasing of blocking effect of confining wall. The slope of curve would decrease with respect to the increasing of jet distance. It means that, the effect of confining wall decrease as jet distance increases. This can be observed in some of the previous works [18, 27].

Figure 5 shows the effect of jet width on the averaged wall heat flux rates. Contrary to the jet distance effect, averaged wall heat flux rates increases as jet width increases. This is because of the increasing the mass flow rate with respect to increasing of jet width.

According to Figures 4 and 5, jet's distance-width ratio is main geometrical parameter affects wall heat flux rates. It is shown in Figure 6. In this figure, results of H effect and W effect are plotted in the same graph. Comparison shows that averaged wall heat flux rate decreases as jet's distance-width ratio increases. It is due to decreasing of coolant mass flow rate and decreasing of confining wall's blocking effect with respect to increasing of jet's distance-width ratio.

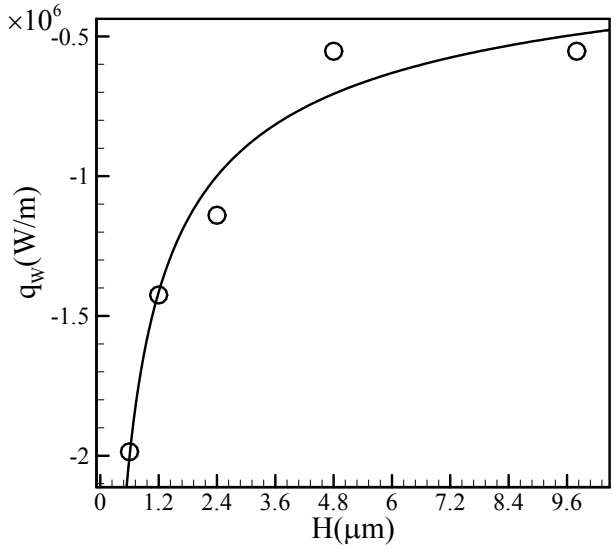

Figure 4. The effects of jet distance from the wall on average heat transfer values, Cases 1-5.

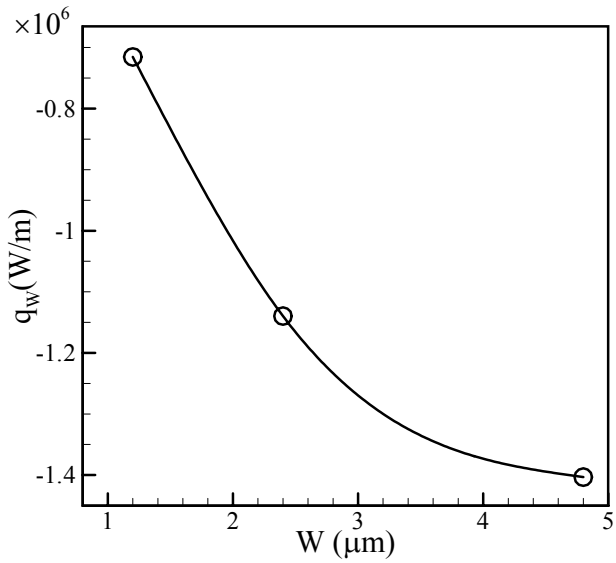

Figure 5. Effect of jet width on the averaged wall heat flux, Cases 6-8.

To magnify the pressure ratio changes on the wall heat flux rates, we study flow behavior with various pressure ratios (Cases 9-13). Figure 7 shows the average wall heat flux rates

and average velocity slip for different pressure ratios from 1.5 to 5. According to the picture, variation of wall heat flux rates is same as that of velocity slips. Hence maximum heat flux rate is relevant to the case with pressure ratio of 1.5 which has minimum velocity slip on the target plate. It is because of this fact that velocity slip on the wall represents the energy level of stroked particles, and heat transfer from the wall would increase as the energy levels of stroked particles decreases.

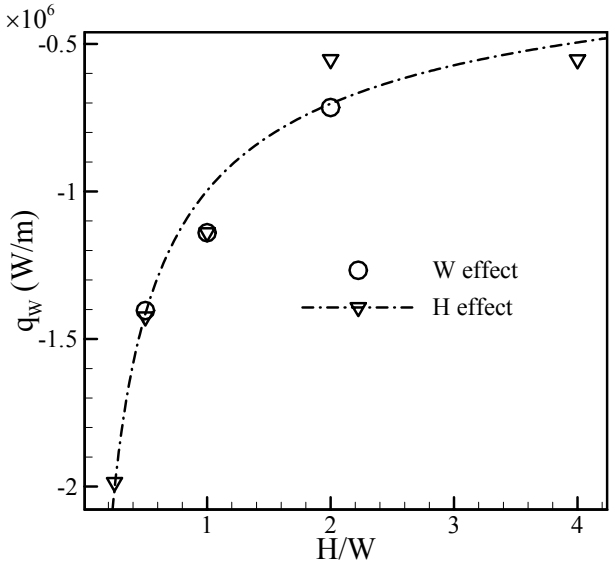

Figure 6. The effects of jet's distance-width ratio on averaged wall heat flux rates, Cases 1-8.

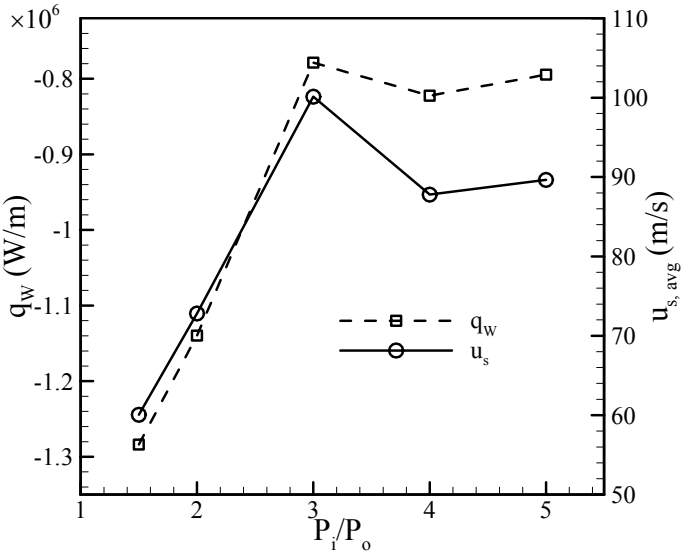

Figure 7. The effects of pressure ratio on the wall heat flux rates and velocity slip, Cases 9-13.

Up to now, all simulation performed under specular base wall and diffusive confining wall. At this point, we want to examine the effects of various wall types on the heat transfer characteristics. For this reason, we apply three wall configurations diffusive, specular, and adiabatic walls (Cases 14-16). In these cases, both of base and confining surfaces have a same wall type. Jet distance from the target wall is considered small to elaborate wall type's effect. Table 1 shows the effects of different wall configurations on averaged values of temperature jump and wall heat flux rate. The results show that the maximum wall heat flux rate is relevant to the diffusive walls which has maximum temperature jump. Some literatures [28, 29] had shown that in rarefied gas flows, temperature jump one if the most important in wall heat flux rates.

Figure 8 shows the temperature fields under different wall types. According to the figure, cases with specular and diffusive walls have the highest and lowest temperature field, respectively. When high energy reflected molecules strike with the confining wall, specular wall preserve molecule's energy, but diffusive wall reduces it, because of the low temperature of the confining wall. Therefore, diffusive and specular walls lead to the highest and lowest values of wall heat flux rates.

Table 2. Averaged values of temperature jump and wall heat flux rate for different wall types, Cases 14-16.

wall types	$T_w - T_j$ (K)	q_W (W/m)
diffusive walls	16	-2.027×10^{-6}
specular walls	3	-0.483×10^{-6}
adiabatic walls	4	-0.847×10^{-6}

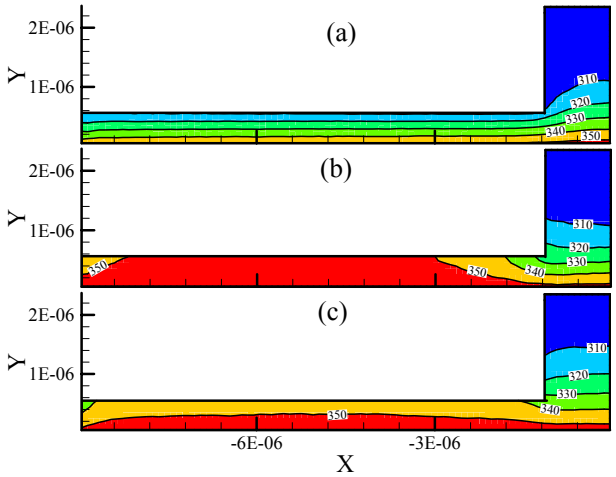

Figure 8. Temperature fields for different wall types, Cases 14-16.

6. CONCLUSION

We studied the rarefied gas flow through a nano slot impinging jet using an extended DSMC solver focusing on heat transfer issue. We considered the effects geometrical parameter, flow condition, and wall types on the flow behavior and wall heat flux rate magnitudes. Our study shows that temperature jump and velocity slip are main parameters affects wall heat flux values. Also, jet's distance-width ratio is the most important geometrical parameter affects heat transfer

characteristics. Case with specular walls, leads to highest temperature field, lowest temperature jump, and lowest wall heat flux values. Additionally, we show that the effect of confining wall becomes weak as jet distance increases.

Nomenclature

AR	Aspect Ratio
c	molecular velocity [m/s]
c_0	mean velocity of simulated molecules [m/s]
c'_m	most probable molecular (thermal) speed [m/s]
U, V	stream velocity components [m/s]
u, v, w	molecular velocity components [m/s]
a	speed of sound [m/s]
M	Mach number
Kn	Knudsen number (Kn= λ /H)
m	molecular mass [Kg]
x, y	Cartesian coordinates [m]
H	channel Height [m]
L	channel Length [m]
n	Total number of simulated molecules that collide the wall during the sampling for each cell
N_0	Number of gaseous molecules associated with one computational molecule
R_f	Random fraction between (0 , 1)
R	gas constant [J/Kg K]
K	Boltzmann constant [Nm/K]
q	heat rate per unit area [W/m^2] (positive sign indicates heat transfer from the fluid to the wall)
P	Pressure [Pa]
T	Temperature [K]

Greek symbols

Δt	time step [s]
Δx	cell sizes in x direction [m]
ϕ	azimuthal parameter
ρ	density [Kg/m^3]
ζ_r	number of rotational degrees of freedom
ε	molecular energy
λ	mean free path [m]

Superscripts, Subscripts and accents

Inc	Incident
ref	reflected
-	Averaged
In	Inlet
Out	Outlet
W	Wall
E	Exit
i, j	cell indexes in x-y directions
B	Back
Tr	Translational
Rot	Rotational
G	Gas

REFERENCES

[1] J. Taylor and C. L. Ren, "Application Continuum Mechanics to Fluid Flow in Nanochannels," *Microfluidics and Nanofluidics*, vol. 1, no. 4, pp. 356–363, Oct. 2005.

[2] V. L. Kovalev and A. N. Yakunchikov, "Flow and Heat Transfer Research in Micro- and Nano- Chnnels," in *WEST-EAST High Speed Flow Field Conf.*, Moscow, Russia, Nov. 19-22, 2007.

[3] M. Raisee, N. Vahedi, and A. Rostamzadeh, "Prediction of Gas Flow through Short and Long 2-D Micro and Nano-Channels Using a Generalized Slip Model". *Proc. of the Sixth International ASME Conference on Nanochannels, Microchannels and Minichannels*, Darmstadt, Germany, June 23-25, 2008.

[4] G.A., Bird, Molecular Gas Dynamics and the Direct Simulation of Gas, Oxford, U.K.: Oxford Science, 1994.

[5] W. Liou and Y. Fang, "Heat Transfer in Microchannel Devices Using DSMC", *Journal of Microelectromechanical Systems*, 10(2), pp. 274-279, 2001.

[6] G.A. Bird, Molecular Gas Dynamics, Clarendon Press, Oxford, 1976.

[7] J. W. Baughn and S. Shim, "Heat Transfer Measurements from a Surface with Uniform Heat Flux and an Impinging Jet", *ASME J. Heat Transfer,* 111, 1096-1098, 1989.

[8] J. W. Baughn, X. J. Yan and M. Mesbah, "The Effect of Reynolds Number on the Heat Transfer Distribution from a Flat Plate to a Turbulent Impinging Jet", *ASME Winter Annual Meeting*, November 1992.

[9] D. Cooper, D. C. Jackson, B. E. Launder, and G. X. Liao, "Impinging Jet Studies for Turbulence Model Assessment-I. Flow-field Experiments", *Int. J. Hear Mass Transfer* 36, 2675-2684, 1993.

[10] Y. J. Craft, L. J. W. Graham and B. E. Launder, "Impinging Jet Studies for Turbulence Model Assessment-II. An Examination of the Performance of Four Turbulence Models", *Int. J. Heat Mass Transfer*, Vol. 36. No. 10. pp. 2685-2697, 1993.

[11] S. Ashforth-frost and K. Jambunathan, "Numerical Prediction of Semi-confined Jet Impingement and Comparison with Experimental Data", *Int. Journal for Numerical Methods in Fluids*, VOL. 23,295-306, 1996.

[12] M. Behnia, S. Parneix, and P. Durbin, "Accurate Predictions of Jet Impingement Heat Transfer", *National Heat Transfer Conference*, Book No H0190, pp. 111-118, 1997.

[13] M. Behina and S. Parneix, "Prediction of Heat Transfer in an Axisymmetric Turbulent Jet Impinging on a Flat Plate", *Int. J. Heat Mass Transfer*. Vol. 41, No. 12, pp. 1845-1855, 1998.

[14] S. Z. Shuja, B. S. Yilbas, and M. O. Budair, "Gas Jet Impingement on a Surface Having a Limited Constant Heat Flux Area: Various Turbulence Models", *Numerical Heat Transfer, Part A: Applications*, 36(2), 171-200, 1999.

[15] A. H. Beirelmal, M. A. Saad, and C. D. Patel "Effects of Surface Roughness on the Average Heat Transfer of an Impinging Air Jet", *Int. Comm. Heat Mass Transfer*, Vol. 27, No. 1, pp. 1-12, 2000.

[16] A. H. Beirelmal, M. A. Saad, and C. D. Patel, "The Effect of Inclination on the Heat Transfer Between a Flat Surface and an Impinging Two-dimensional Air Jet", *International Journal of Heat and Fluid Flow,* 21, 156-163, 2000.

[17] C. Glynn and D. B. Murray, "Jet Impingement Cooling in Microscale", *ECI International Conference on Heat Transfer and Fluid Flow in Microscale Castelvecchio Pascoli*, 25-30, September 2005.

[18] V. Katti and S.V. Prabhu, "Experimental Study and Theoretical Analysis of Local Heat Transfer Distribution Between Smooth Flat Surface and Impinging Air Jet from a Circular Straight Pipe Nozzle", *International Journal of Heat and Mass Transfer,* 51, 4480–4495, 2008.

[19] Y. Ozmen, E. Baydar, "Flow structure and heat transfer characteristics of an unconfined impinging air jet at high jet Reynolds numbers", *Heat Mass Transfer* 44:1315–1322, 2008.

[20] T.L. Lupton, D.B. Murray, and A.J. Robinson, "The Effects of Varying Confinement Levels on the Heat Transfer to a Miniature Impinging Air Jet", *5th European Thermal-Sciences Conference*, The Netherlands, 2008.

[21] K. S. Choo, Y. J. Youn, S. J. Kim, and D. H. Lee, "Heat Transfer Characteristics of a Micro-scale Impinging Slot Jet", *International Journal of Heat and Mass Transfer* 52, 3169-3175, 2009.

[22] U. Kursun and J. Kapat, "Numerical Simulation of Microscale Slot Jet Impingement Cooling of a Surface With Constant Heat Flux Using DSMC-IP", *Proc. of the sixth international ASME Conference on Nanochannels, Microchannels and Minichannels*, Darmstadt, Germany, June 23-25. ICNMM2008-62354, 2008.

[23] M. Wang and L. Zhixin, "Simulation for Gas Flow in Microgeometries Using the Direct Simulation Monte Carlo Method". *International Journal of Heat and Fluid Flow*, 25, pp. 975–985, 2004.

[24] Y. Fang and W. W. Liou, "Computations of the Flow and Heat Transfer in Microdevices Using DSMC with Implicit Boundary Conditions". *Journal of Heat Transfer*, Vol. 124, pp. 338-345, 2002.

[25] W. W. Liou and Y. C. Fang, "Implicit Boundary Conditions for Direct Simulation Monte Carlo Method in MEMS Flow Predictions". *Computer Modeling in Engineering & Science*, 1(4), pp. 119-128, 2000.

[26] Q. Wang, X. Yan, and Q. He, "Heat-flux-specified Boundary Treatment for Gas Flow and Heat Transfer in Microchannel Using Direct Simulation Monte Carlo Method", *Int. J. Numer. Meth. Engng,* 74:1109–1127, 2008.

[27] S. Wu, J. Mai, and Y. C. Ho "Micro Heat Exchanger by Using MEMS Impinging Jet". Proc. IEEE, pp. 171-176, 1999.

[28] M. Darbandi and H. Akhlaghi, "Heat Transfer in Nanochannel Devices Using DSMC", *Proc. of the 3rd Conference on Nanostructures (NS2010)*, March 10-12, Kish Island, I.R. Iran, NS2010-G288, 2010.

[29] M. Darbandi, H. Akhlaghi, and G.E. Schneider, "The Effects of Wall Temperature on the Heat Transfer Characteristics of Supersonic Flows through Micro/Nano Devices", *Int. Con. on Computational & Experimental Engineering & Sciences, ICCES'10*, Las Vegas, USA, March 28-April 1, ICCES1020100304395, 2010.